Super-Resolution Simplified: Sub-10nm Imaging Over Large Areas and Deep Penetration via SDC-OPR and DNA-PAINT

Cecilia Zaza[1], Megan D. Joseph[1], Olivia P. L. Dalby[1,2], Rhian F. Walther[3], Karol Kołątaj[4,5] Germán Chiarelli[4], Franck Pichaud[3,6], Guillermo P. Acuna[4,5] and Sabrina Simoncelli[1,2]*

1. London Centre for Nanotechnology, University College London, 19 Gordon Street, WC1H 0AH London, United Kingdom.

2. Department of Chemistry, University College London, 20 Gordon Street, WC1H 0AJ London, United Kingdom.

3. Laboratory for Molecular Cell Biology, University College London, London WC1E 6BT, UK

4. Department of Physics, University of Fribourg, Chemin du Musée 3, Fribourg CH 1700, Switzerland

5. Swiss National Center for Competence in Research (NCCR) Bio-inspired Materials, University of Fribourg, Chemin des Verdiers 4, CH-1700 Fribourg, Switzerland

6. Institute for the Physics of Living Systems, University College London, London WC1E 6BT, UK

ABSTRACT

Single molecule localization microscopy (SMLM) is constrained by selective illumination configurations to achieve high signal-to-background ratio (SBR), forcing trade-offs between penetration depth, field-of-view (FOV), and spatial resolution. We demonstrate that a Spinning Disc confocal microscope with Optical Photon Reassignment (SDC-OPR) in combination with DNA-PAINT effectively balances these limitations. This system enables high-resolution imaging through multiple cellular layers, enhancing spatial resolution while remaining practical and accessible for diverse biological applications.

MAIN

The most widely used approach for SMLM[1] is in combination with wide-field illumination, under total internal reflection (TIR)[2] or highly inclined and laminated

optical sheets (HILO) excitation[3], achieving a lateral localization precision (σ_{SMLM}) below 5 nm[4,5] with DNA-PAINT[6]. However, this comes at the expense of limited penetration depth, < 250 nm for TIR, and a reduced field-of-view of ~40 × 10 μm^2 for HILO[7,8]. SMLM can also be implemented in confocal setups, including point-scanning and spinning disk confocal (SDC), which enable deeper sample penetration[9], making it preferable for imaging tissue samples. Image Scanning Microscopy (ISM)[10] doubles the spatial resolution of confocal microscopy[11,12] via pixel reassignment and, when combined with SMLM, has recently achieved a σ_{SMLM} of 8 nm, though with a small FOV of 8 × 8 μm^2 [13]. To increase acquisition speed and FOV size, SDC employs hundreds of spiraled pinholes on a rotating disc, coupled with a camera instead of a single-point detector. SDC configurations have been adapted for SMLM, achieving a planar localization precision of 8 nm with DNA-origami samples and 22 nm for cells in the basal plane using DNA-PAINT[14]. Still, as the emission light is blocked by the disc, the achievable resolution remained limited due to reduced excitation intensity. In 2015, Azuma and colleagues proposed an enhanced SDC with optical photon reassignment (SDC-OPR)[15], an array of microlenses to improve resolution by effectively reducing the pinhole size and increasing photon collection. These microlenses contract the focus twofold, directing emitted photons back to their probable origin points (Fig. 1a). Therefore, this raises the question: can SDC-OPR outperform current optical configurations, overcoming the trade-offs between penetration depth, field-of-view, and spatial resolution? In this Brief Communication, we show that SMLM on a SDC-OPR fluorescence microscope can achieve sub-2 nm localization precision in the basal plane and sub-10 nm up to 7 μm penetration depth within a FOV of 53 × 53 μm^2 using a commercially available SDC-OPR (CSU-W1 SoRA Nikon system). The power of the SDC-OPR is highlighted by visualizing, with unprecedented resolution, adherents junctions in the retinal epithelium of the eye imaginal disc of Drosophilas.

To evaluate the spatial resolution achievable with SMLM on an SDC-OPR system, we designed 2D DNA-origami nanostructures for DNA-PAINT imaging. These structures feature three pairs of DNA docking strands spaced 53 nm apart, with edge pairs separated by 10 nm and the central pair by 17 nm, as illustrated in Fig. 1b. DNA-PAINT on a standard SDC achieved an average localization precision of 10 nm consistent with previous studies[14], and could not resolved individual docking strands spaced 10 nm apart (Fig. 1c and Extended Data Fig. 1 for representative individual DNA-origami structures). However, DNA-PAINT imaging on an SDC-OPR successfully resolved these strands, both separated by 17 nm and 10 nm across all DNA-origami structures within the FOV (Fig. 1c and Extended Data Fig. 2). We measured an average distance of 17 ± 1 nm and 9.8 ± 0.5 nm between central and edge docking strand pairs, respectively (n = 60 origamis), consistent with our observations under TIR illumination (Extended Data Fig. 3). Notably, the SDC-OPR achieved an exceptional localization precision of 1.8 nm and 5 nm resolution calculated by nearest-neighbour-based metric (NeNA)[16] with an image acquisition time of 75 minutes over a 53 × 53 μm² FOV. A similar σ_{SMLM} can be maintained for 76 × 76 μm² FOVs, though it increases to 10 nm for 211 × 211 μm² due to reduced

excitation power density (see Fig. 1d and Extended Data Fig. 4 and 5 for images and quantitative information under different imaging conditions). These results demonstrate an unprecedented level of resolution in confocal-based optical microscopy, capable of distinguishing structures closer than 10 nm.

To illustrate the enhanced resolution achieved with an SDC-OPR in a cellular context, we imaged the structural proteins of the nuclear pore complex (NPC) in HeLa cells. NPCs were selected as a model system due to their stereotypic protein arrangement, often used to benchmark super-resolution fluorescence microscopy[17]. Figure 1e shows a DNA-PAINT SDC-OPR image of Nup107, tagged with monomeric enhanced green fluorescent proteins (mEGFPs) and labelled with DNA-conjugated anti-GFP nanobodies. Nup107, a structural protein of the NPC's Y-complex, is present in eight pairs on both the cytoplasmic and nuclear rings, totalling 32 copies per NPC. In this work, we imaged the cytoplasmic ring, where individual Nup107 protein pairs are spaced 13.5 nm laterally and 5.3 nm axially (Fig. 1f). Zooming in on selected NPCs (Fig. 1g and Extended Data 6) reveals distinct pairs of closely spaced Nup107 proteins (indicated by arrows in Fig. 1g). We measured the Euclidean distance between Nup107 pairs by aligning them and plotting a cross-sectional histogram of the summed image (Fig. 1g, n = 26 pairs). This reveals a peak-to-peak distance of (13 ± 2) nm, consistent EM models[18] and HILO imaging results[19] (Extended Data 7). Additionally, each peak fit exhibits a standard deviation of 1 nm, confirming the high localization precision of 2 nm achieved with DNA-PAINT imaging on the SDC-OPR system.

After demonstrating the exceptional resolution achieved on the SDC-OPR system, we assessed its performance as a function of the FOV and penetration depth. Figure 2a displays a DNA-PAINT image of the microtubule network in fixed HeLa cells, labelled with primary DNA-conjugated antibodies targeting alpha-tubulin. Captured at the SDC-OPR's lowest magnification (1×, 211 × 211 μm² FOV) and an average localization precision of 9.5 nm, this image illustrates the method's capability of high-resolution SMLM imaging across multiple cells (>10 HeLa cells) in a single image, enabling researchers to tackle questions of heterogeneity (Fig. 2a, lower panel). For depth-dependent analysis, we acquired DNA-PAINT images of a confocal volume of ~500 nm thickness using the system highest magnification (4×, 53 × 53 μm² FOV). This volume was sequentially imaged in 1-μm steps throughout the cell's 9 μm height (see Fig. 2b and Extended Data Fig. 8). We found that double-walled filamentous microtubule structures were clearly resolved at various depths: near the coverslip–cell interface, at intermediate axial positions, and at the top of the cell (Fig. 2c), with an average peak-to-peak distance between 30 nm and 40 nm, consistent with reported values[20]. These results highlight the SDC-OPR's ability to deliver high-resolution images across large field-of-views and throughout the entire height of cells.

To demonstrate the power and ease of SMLM imaging on a SDC-OPR system for the biology community, we imaged retinal cell adherens junctions (AJs) in the Drosophila eye imaginal disc, labelled with GFP-tagged E-cadherin[21]. The eye disc comprises a

thin squamous epithelium, the peripodial membrane (ppm), overlying the retinal epithelium made of columnar cells (Fig. 2d). In flies, the epithelial AJ is found at the border of apical and lateral domains of cells. For imagining, we mounted the eye discs with the ppm facing the objective, requiring imaging through both the ppm and luminal space. Figure 2e presents a color-coded z-projection of E-cadherin through these layers, showing continuous staining at the AJs. E-cadherin is known to be enriched between differentiating photoreceptor neurons and less abundant in progenitor cells destined to become pigment and accessory cells[22]. Switching to DNA-PAINT revealed a more detailed E-cadherin distribution at the AJs, with high-intensity foci and a heterogeneous pattern in both ppm and retinal cells. Notably, DNA-PAINT allowed us to image AJs in the retinal epithelium, 6 to 9 µm below the surface of the ppm, confirming the SDC-OPR capability to accurately image through multiple layers. This enhanced spatial resolution also confirmed a heterogeneous E-cadherin distribution at the AJs, consistent with previous observations in other developing epithelia[23]. At this point, it is important to highlight that super-resolved imaging of tissues with such low localization precision across various penetrations depth is limited[24] due to the challenges in imaging at greater depths, combined with high dispersion inherent of tissue structures. The unprecedented resolution obtained using the SDC-OPR in the eye imaginal disc underscores its transformative potential to enable researchers to explore subcellular structures in complex tissue environments with remarkable resolution.

In summary, we introduce the integration of DNA-PAINT, a single molecule localization microscopy (SMLM) technique, with a commercially available Spinning Disc Confocal microscope with Optical Photon Reassignment (SDC-OPR). This combination achieves sub-2 nm localization precision within 53 × 53 μm^2 field-of-view in the basal plane, sub-10 nm up to 7 µm penetration depth. For larger FOVs (211 × 211 μm^2) localization precision remains around 10 nm. While recent advancements in lattice light-sheet (minimum σ_{SMLM} of 28 nm)[25] and 4Pi microscopy (between 10 and 20 nm resolution)[26] allow for larger FOVs and deeper penetration, SDC-OPR microscopy offers a more accessible and user-friendly alternative. It provides high-resolution imaging with a relatively simple setup, making it an excellent choice for a wide range of biological applications, balancing practically with performance for investigating different biological questions.

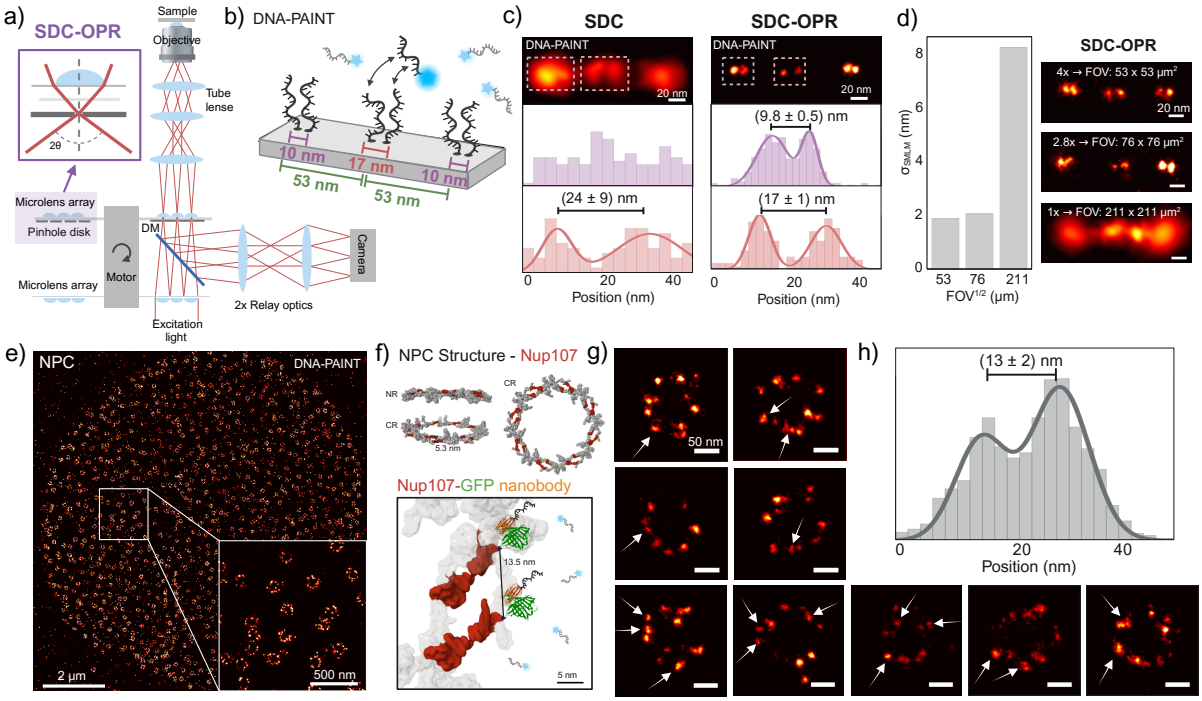

Figure 1. (a) Schematic diagram of SDC-OPR (CSU-W1 SoRA Nikon system) optical setup, showing the added microlenses array, which contracts the emission collected by the objective for better coupling to the pinholes. (b) Diagram of DNA-origami used in the experiments, featuring 6 sites with docking strands for DNA-PAINT. (c) Super-resolved image of one DNA-origami structure (b) imaged with the SDC (left) and SDC-OPR (right) setup. Lower panels display the position distribution and measured distances of left and central pair docking sites. (d) Localization precision (σ_{SMLM}) for the DNA-origami sample across different FOV sizes, with a representative and one super-resolved DNA-origami image for each magnification. (e) DNA-PAINT overview image of NPC in Hela cells with a zoomed-in-view highlighting the arrangement of Nup107 in NPCs. (f) Cryo-EM structure representation of Nup107 proteins (red) in NPCs (grey) adapted from PDB 7PEQ[27]. (g) Selection of single NPCs with arrows highlighting pairs of Nup107 proteins within the same symmetry center. (h) Cross-sectional histogram of average protein pairs (n=26) in single symmetry centers, showing a 13 nm distance between single proteins.

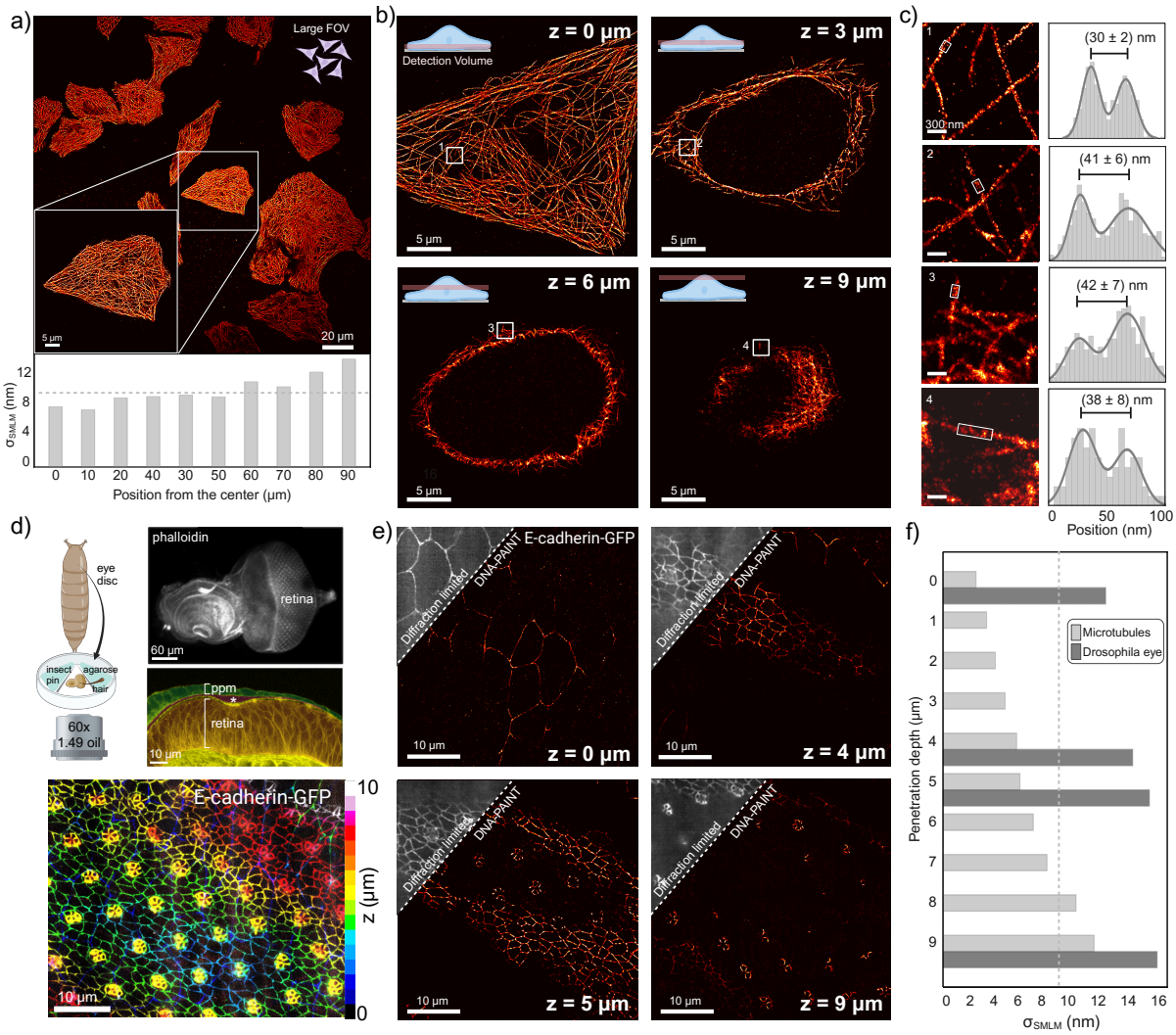

Figure 2. (a) DNA-PAINT overview of microtubules in HeLa cells across a 211µm × 211 µm^2 field-of-view (FOV) with a zoomed-in view of one of the cells. The lower panel displays localization precision (σ_{SMLM}) at different FOV positions to assess image homogeneity. (b) DNA-PAINT images of microtubules at different penetration depths. (c) Left: Zoomed-in image of the highlighted areas in (b). Right: Position distribution of the highlighted regio, showing the distances between microtubules wall for different penetration depths. (d) Right: Schematic of the 3rd instar Drosophila eye disc and the sample mounting method used to prevent drift during acquisition. Left: Phalloidin staining of the eye disc (top). The peripodial membrane (ppm), the luminal space (*), and the retinal epithelium (retina) are highlighted with green, magenta, and orange masks, respectively (bottom). (e) DNA-PAINT images of the tissue at different penetration depths. (f) Localization precision (σ_{SMLM}) as a function of the penetration depth for the microtubules and Drosophila eye disc sample.

Funding Sources

This research was funded by the Human Frontier Science Program Organization (HFSP) through a cross-disciplinary post-doctoral fellowship to CZ (LT0025/2023-C), the Engineering and Physical Sciences Research Council (EP/R513143/1 and EP/T517793/1), the Biotechnology and Biological Sciences Research Council through the London Interdisciplinary Doctoral Programme to MDJ (BB/T008709/1) and the Royal Society through a Dorothy Hodgkin fellowship to SS (DHF\R1\191019). FP lab is funded by the MRC, MR/V001256/1 and M/Y012089/1 to FP, and the BBSRC, BB/Y002075/1 to FP and RWW. G.P.A. acknowledges support from the Swiss National Science Foundation (200021_184687) and through the National Center of Competence in Research Bio-Inspired Materials (NCCR, 51NF40_182881), the European Union Program HORIZON-Pathfinder-Open: 3D-BRICKS, grant Agreement 101099125. This work has also been supported by The Chan Zuckerberg Initiative “Multi-color single molecule tracking with lifetime imaging” (2023-321188).

Acknowledgement

M.D.J. acknowledges support from the London Interdisciplinary Doctoral Programme. O.P.L.D acknowledges financial support from the Engineering and Physical Sciences Research Council. C. Z. acknowledges financial support from the Frontier Science Program Organization. S.S. acknowledges financial support from the Royal Society.

References

1. Lelek, M. *et al.* Single-molecule localization microscopy. *Nature reviews methods primers* **1**, 39 (2021).
2. Axelrod, D. Cell-substrate contacts illuminated by total internal reflection fluorescence. *J Cell Biol* **89**, 141–145 (1981).
3. Tokunaga, M., Imamoto, N. & Sakata-Sogawa, K. Highly inclined thin illumination enables clear single-molecule imaging in cells. *Nat Methods* **5**, 159–161 (2008).
4. Raab, M., Schmied, J. J., Jusuk, I., Forthmann, C. & Tinnefeld, P. Fluorescence microscopy with 6 nm resolution on DNA origami. *ChemPhysChem* **15**, 2431–2435 (2014).
5. Schnitzbauer, J., Strauss, M. T., Schlichthaerle, T., Schueder, F. & Jungmann, R. Super-resolution microscopy with DNA-PAINT. *Nat Protoc* **12**, 1198–1228 (2017).
6. Jungmann, R. *et al.* Single-molecule kinetics and super-resolution microscopy by fluorescence imaging of transient binding on DNA origami. *Nano Lett* **10**, 4756–4761 (2010).
7. Gardini, L., Vignolini, T., Curcio, V., Pavone, F. S. & Capitanio, M. Optimization of highly inclined illumination for diffraction-limited and super-resolution microscopy. *Opt Express* **31**, 26208–26225 (2023).
8. Vignolini, T., Capitanio, M., Caldini, C., Gardini, L. & Pavone, F. S. Highly inclined light sheet allows volumetric super-resolution imaging of efflux pumps distribution in bacterial biofilms. *Sci Rep* **14**, 12902 (2024).

9. Pawley, J. *Handbook of Biological Confocal Microscopy*. vol. 236 (Springer Science & Business Media, 2006).
10. Müller, C. B. & Enderlein, J. Image scanning microscopy. *Phys Rev Lett* **104**, 198101 (2010).
11. Zaza, C. *et al.* Super-Resolved FRET Imaging by Confocal Fluorescence-Lifetime Single-Molecule Localization Microscopy. *Small Methods* **7**, 2201565 (2023).
12. Oleksiievets, N. *et al.* Fluorescence lifetime DNA-PAINT for multiplexed super-resolution imaging of cells. *Commun Biol* **5**, 38 (2022).
13. Radmacher, N. *et al.* Doubling the resolution of fluorescence-lifetime single-molecule localization microscopy with image scanning microscopy. *Nat Photonics* 1–8 (2024).
14. Schueder, F. *et al.* Multiplexed 3D super-resolution imaging of whole cells using spinning disk confocal microscopy and DNA-PAINT. *Nat Commun* **8**, 2090 (2017).
15. Azuma, T. & Kei, T. Super-resolution spinning-disk confocal microscopy using optical photon reassignment. *Opt Express* **23**, 15003–15011 (2015).
16. Endesfelder, U., Malkusch, S., Fricke, F. & Heilemann, M. A simple method to estimate the average localization precision of a single-molecule localization microscopy experiment. *Histochem Cell Biol* **141**, 629–638 (2014).
17. Thevathasan, J. V. *et al.* Nuclear pores as versatile reference standards for quantitative superresolution microscopy. *Nat Methods* **16**, 1045–1053 (2019).
18. Petrovic, S. *et al.* Architecture of the linker-scaffold in the nuclear pore. *Science (1979)* **376**, eabm9798 (2022).
19. Schlichthaerle, T. *et al.* Direct visualization of single nuclear pore complex proteins using genetically-encoded probes for DNA-PAINT. *Angewandte Chemie* **131**, 13138–13142 (2019).
20. Stehr, F., Stein, J., Schueder, F., Schwille, P. & Jungmann, R. Flat-top TIRF illumination boosts DNA-PAINT imaging and quantification. *Nat Commun* **10**, 1268 (2019).
21. Huang, J., Zhou, W., Dong, W., Watson, A. M. & Hong, Y. Directed, efficient, and versatile modifications of the Drosophila genome by genomic engineering. *Proceedings of the National Academy of Sciences* **106**, 8284–8289 (2009).
22. Robertson, F., Pinal, N., Fichelson, P. & Pichaud, F. Atonal and EGFR signalling orchestrate rok-and Drak-dependent adherens junction remodelling during ommatidia morphogenesis. *Development* **139**, 3432–3441 (2012).
23. Cavey, M., Rauzi, M., Lenne, P.-F. & Lecuit, T. A two-tiered mechanism for stabilization and immobilization of E-cadherin. *Nature* **453**, 751–756 (2008).
24. Schueder, F. *et al.* Nanobodies combined with DNA-PAINT super-resolution reveal a staggered titin nanoarchitecture in flight muscles. *Elife* **12**, e79344 (2023).
25. Legant, W. R. *et al.* High-density three-dimensional localization microscopy across large volumes. *Nat Methods* **13**, 359–365 (2016).
26. Huang, F. *et al.* Ultra-high resolution 3D imaging of whole cells. *Cell* **166**, 1028–1040 (2016).
27. Schuller, A. P. *et al.* The cellular environment shapes the nuclear pore complex architecture. *Nature* **598**, 667–671 (2021).
28. Douglas, S. M. *et al.* Rapid prototyping of 3D DNA-origami shapes with caDNAno. *Nucleic Acids Res* **37**, 5001–5006 (2009).

29. Poppleton, E., Mallya, A., Dey, S., Joseph, J. & Šulc, P. Nanobase. org: a repository for DNA and RNA nanostructures. *Nucleic Acids Res* **50**, D246–D252 (2022).
30. Xu, K., Zhong, G. & Zhuang, X. Actin, spectrin, and associated proteins form a periodic cytoskeletal structure in axons. *Science (1979)* **339**, 452–456 (2013).
31. Li, Y. *et al.* Real-time 3D single-molecule localization using experimental point spread functions. *Nat Methods* **15**, 367–369 (2018).
32. Corrigall, D., Walther, R. F., Rodriguez, L., Fichelson, P. & Pichaud, F. Hedgehog signaling is a principal inducer of Myosin-II-driven cell ingression in Drosophila epithelia. *Dev Cell* **13**, 730–742 (2007).

METHODS

DNA origami synthesis

The rectangular DNA origami structure with a pillar in the center (Fig 1b) was designed using CaDNAno[28] and it is accessible at https://nanobase.org/structure/146[29]. It is modified with six biotin staples going out of the structure for binding to the surface, 3 pairs of DNA Paint docking strands (TCCTCCTCCTCCTCCTCCT and ACACACACACACACACACA) and two fixed dyes (ATTO 532 and ATTO 647N) at two ends of the structure. It is based on a 7249-nucleotide long scaffold extracted from the M13mp18 bacteriophage (Tilibit Nanosystems GmbH) and folded into the desired shape using 243 staples folded in 1x TAE (Alfa Aesar, #J63931) and 12 mM $MgCl_2$ (Alfa Aesar, #J61014) buffer. It was mixed in a 10-fold excess of staples over scaffold, and 100-fold for especially modified staples.

Unmodified staple strands were purchased from IDT; biotin-functionalized staples, dye-labeled staple strands with ATTO 532 and ATTO 647N as well as DNA-PAINT docking strands were purchased from Biomers GmbH. The fluorophores used here are linked through a C6-linker to the single-stranded DNA to the 3'-end. The scaffold and the staple mix were self-assembled into the designed structure using a temperature ramp. The combination was initially heated to 95 C°, where it remained for 5 minutes, before being cooled to 20 C° during a 19 hs linear ramp. A 1% agarose gel electrophoresis was used as a purification procedure to remove excess of staple strands. In a 1× TAE 12 mM $MgCl_2$ buffer, the gel was run at 70V for 3 h in an ice-water bath. After electrophoresis, the pure DNA-origami structures were extracted by cutting out the bands in the gel containing the DNA-origami structure and squeezing the out using a parafilm-wrapped glass slide. The final concentration of the DNA-origami structures was determined on a Nanodrop 2000 spectrophotometer (Thermo Fisher Scientific).

Buffers

Buffer A+: 10 mM Tris (VWR) pH 8.0, 100 mM NaCl (Sigma-Aldrich) and 0.05% Tween-20 (Sigma-Aldrich)

Buffer B+: 10 mM $MgCl_2$ (LifeTech), 5 mM Tris-HCl pH 8.0, 1 mM EDTA (LifeTech) and 0.05% Tween-20 (Sigma-Aldrich) pH 8.0, optionally supplemented with 1× trolox, 1× PCA and 1× PCD

Buffer C+: 1× PBS, 1 mM EDTA (Invitrogen), 500 mM NaCl (Sigma-Aldrich) pH 7.4, 0.02% Tween (Sigma-Aldrich), optionally supplemented with 1× trolox, 1× PCA and 1× PCD

PCA, PCD and Trolox: To summarise, this system consisted of 1× protocatechuic acid (PCA, stock 40x solution), 1× protocatechuate 3,4-dioxygenase (PCD, stock 100× solution) and 1× (±)-6-Hydroxy-2,5,7,8-tetramethylchromane-2-carboxylic acid (Trolox, stock 100× solution) in 1× PBS + 500 mM NaCl buffer and incubated in the dark for 1 h before imaging. 40x PCA stock was made from 154 mg of PCA (Sigma-Aldrich) in 10 ml of distilled water adjusted to pH 9.0 with NaOH (Avantor). 100× PCD solution was made by adding 2.2 mg of PCD (Sigma-Aldrich) to 3.4 ml of 50% glycerol (Sigma-Aldrich) with 50 mM KCl (Sigma-Aldrich), 1 mM EDTA (Invitrogen) and 100 mM Tris buffer (VWR). 100× Trolox solution was made by dissolving 100 mg of Trolox (Sigma-Aldrich) in 0.43 ml methanol (Sigma-Aldrich), 0.345 ml 1 M NaOH and 3.2 ml of distilled water.

Cytoskeleton Buffer (CB): 10 mM MES (Sigma-Aldrich), pH 6.1, 150 mM NaCl (Sigma-Aldrich), 5 mM EGTA (Sigma-Aldrich), 5 mM D-glucose (LifeTech), 5 mM $MgCl_2$ (LifeTech); described in ref[30].

DNA-origami sample preparation

For sample immobilization, commercial chambers (IB-80607 | μ-Slide VI 0.5 Glass Bottom, Sterile) were used. The surface was passivated with BSA biotin (1 mg/mL^{-1}, A4503-10G, SigmaAldrich) for 20 minutes at room temperature on top of a rotating platform. After 3 washes with buffer A+, slides were incubated with neutravidin (1 mg/mL^{-1}, no. 31000 Thermo Fisher Scientific) diluted in buffer A+ and incubated for 20 min at room temperature on a rotation platform. After an additional wash with buffer B+, 100 pM of DNA-origami structure was added to the chamber and incubated for 15 min for immobilization via biotin binding to the functionalized surface. The sample was washed again with buffer B+ and 100 μl of gold nanoparticles (90 nm, no. G-90-100, Cytodiagnostics) was flushed through and incubated for 5 min before washing with buffer B+. Finally, 180 μl of imager solution in buffer B+ supplemented with 1× trolox, 1× PCA and 1× PCD was flushed into the chamber for imaging.

Antibody–DNA conjugation

An antibody against α-tubulin (MA1-80017 (YL1/2), Thermo Fisher Scientific) was conjugated to DNA-PAINT docking strand R2 5′-Thiol-AAACCACCACCACCACCACCA-3′ (Custom, Eurofins) via maleimidePEG2-succinimidyl ester coupling reaction. In brief, 1 mM thiolated DNA docking strand was reduced with freshly prepared 250 mM DTT (Thermo Fisher Scientific) solution for 2h at room temperature. The α-tubulin antibody was then concentrated using 100kDa Amicon spin filter (Merck/EMD Millipore) before mixing with 20x molar excess of maleimide-PEG2-succinimidyl ester cross-linker (Sigma-Aldrich) for 90 min at 4 °C in the dark. To remove excess DTT and cross-linker, the reactions were purified by spin filtration using a Microspin Illustra G-25 column (GE Healthcare) and a Zeba spin desalting column (7K MWCO, Thermo Fisher Scientific), respectively. The reduced DNA docking strand was added to the purified α-tubulin-crosslinker solution at 10x molar excess and incubated on a shaker overnight at 4°C in the dark. Finally, excess DNA was removed from the α-tubulin product via 100kDa Amicon spin (Merck/EMD Millipore) filtration and stored at 4ºC. Antibody-DNA concentration was measured using a NanoDrop One spectrophotometer (Thermo Fisher Scientific), with the final ratio of DNA:antibody measured to be 1.3.

Cell culture

HeLa Kyoto mEGFP-Nup107 were cultured in Dulbecco's Modified Eagle Medium (DMEM) supplemented with 10 % Foetal Bovine Serum (FBS) and 1 % Penicillin with Streptomycin (P/S). Cells were maintained at 2×10^5 cells/ml and passaged using trypsin-EDTA.

Nup107 EGFP and alpha tubulin labelling

24 hours prior to imaging 2×10^4 (2×10^5 cells/ml) HeLa Kyoto mEGFP-Nup107 cells were seeded in 8 well ibidi microslides (IB-80807) in supplemented DMEM media as described above.

For Nup107 imaging, media was then exchanged with phosphate buffered saline (PBS) and cells were fixed using 4 % paraformaldehyde (PFA) for 30 minutes. Permeabilization was then achieved via addition of 0.1 % Triton X-100 for 5 minutes. Samples were washed 3 × 3min in 60 mM Glycine in PBS to quench autofluorescence. Blocking was done through the addition of 5 % Bovine Serum Albumin (BSA) for 60 minutes in the dark. 20 nM DNA coupled anti-GFP nanobody (Massive-sdAB-FAST 2-Plex, Massive Photonics GmbH) in 5 % BSA was added for one hour at room temperature. Samples were washed 3 × 3min with PBS before the addition of 90 nm gold nanoparticles (no. G-90-100, Cytodiagnostics) for 5 minutes. For imaging, 1 nM DNA imager solution (F3: Cy3B from Massive-sdAB-FAST 2-Plex, Massive Photonics

GmbH) with 3' attached Cy3b fluorophore in C+ buffer supplemented with 1× Trolox, 1× PCA and 1× PCD was added before imaging.

For microtubule imaging the protocol was adapted from ref[31]. After the overnight incubation, most of the cell culture medium was aspirated using a glass pipette placed carefully into a corner of each chamber. Simultaneously, 200 µl of 0.3% (v/v) glutaraldehyde in Cytoskeleton Buffer (CB) + 0.25% (v/v) Triton X-100 is added down the side of the chamber using a second pipette. This prefixation solution is kept for 2 minutes. Then, cells are fixed with 2% (v/v) glutaraldehyde in CB for 10 min. Auto-fluorescence was quenched with 3 × 3min of Glycine 60 mM in PBS. 5 µg/ml of the coupled anti-alpha tubulin antibody (described in Antibody–DNA conjugation section) in 2 % BSA was added for 2 hours at room temperature. Samples were washed 3 × 3min with PBS. For imaging, 1 nM DNA imager solution (R2: 5'-TGGTGGT-3') 3' attached Cy3b fluorophore in C+ buffer was added before imaging.

Third instar eye discs

Third instar eye discs were dissected as previously described[32] from transgenic flies where the endogenous E-Cadherin locus has been tagged with GFP[21]. Discs were incubated with 20 nM GFP antibody (Anti-GFP Custom docking site (sdAB-5'-TCCTCCTCCTCCT-3'), Massive Photonics GmbH) in PBS + 0.3% Triton overnight at 4 degrees. Alexa Fluor Plus 405 phalloidin (Thermofisher A30104) was added at 165 nM for 2-4 hours at room temperature. Samples were washed 3× and left overnight at 4ºC. Immediately before imaging, the wash was replaced with 10 nM DNA imager solution (R1: 5'-AGGAGGA-3') 3' attached Cy3b fluorophore in C+ buffer supplemented with 1× Trolox, 1× PCA and 1× PCD.

Discs were imaged in modified 35mm glass bottomed dishes. Three insect pins (Fine Science Tools 26002-20) were arranged as a triangle and glued in place over two human hairs using superglue (cyanoacrylate) (Extended Data Fig. 9). A central, triangular chamber with two sections was formed, each having an end of one hair free. 2% agarose was added to the outer sections of the coverglass to minimise the chamber volume. After five minutes, imaging solution was added to the chamber. Two discs were pipetted, each into a section of the triangular chamber, placing each eye disc under a hair to immobilize them (Fig. 1d).

Microscopy setups

TIR setup: TIR microscopy was carried out on a custom built total internal reflection fluorescence microscope based on a Nikon Eclipse Ti-2 microscope equipped with a 100× oil immersion TIRF objective (Apo TIRF, NA 1.49) and a Perfect Focus System. Samples were imaged under flat-top TIRF illumination with a 560 nm laser (MPB Communications, 1 W) magnified with both a custom-built telescope and a variable

beam expander, before passing through a beam shaper device (piShaper 6_6_VIS, AdlOptica, Berlin, Germany) to transform the Gaussian profile of the beam into a collimated flat-top profile. Laser polarization was adjusted to circular using a polarizer followed by a quarter waveplate. The beam was focused into the back focal plane of the microscope objective using a suitable lens, passed through a excitation filter (FF01-390/482/563/640-25, Semrock) and coupled into the objective using a beam splitter (Di03- R405/488/561/635 , Semrock). Fluorescence light was spectrally filtered with an emission filter (FF01-446/523/600/677-25, Semrock) and imaged on a sCMOS camera (Hamamatsu, ORCA-Fusion BT) without further magnification, resulting in a final pixel size of 130 nm in the focal plane, after 2 × 2 binning.

SCD-OPR setup: This is a commercial setup CSU-W1 SoRA from Nikon. Multifocal laser excitation is generated by micro-array lenses on the upper disk of the scanning unit. This excitation passes through a corresponding array of pinholes on the lower disk of the scanning unit. The multifocal excitation then scans the specimen through a tube lens and an objective lens. The lower disk also contains micro-array lenses on the underside which focuses the fluorescence emission from the sample by twofold. This displaces emitted photons to their most probable original location, mimicking the effect of an infinitely small pinhole size without compromising brightness. Pinholes further reject out-of-focus emissions to achieve the enhancement in resolution whilst maintaining confocal sectioning. This emission is then reflected by a dichroic mirror and imaged by an ORCA-Fusion BT Digital CMOS camera through magnifying relay optics and emission filters. The SoRA element is added onto a Nikon Ti2 inverted microscope base which has a dual camera function. Magnification on the SDC-OPR can be 1×, 2.8× and 4×, resulting in a pixel size of 108 nm (with no binning), 78 nm (with 2× binning) and 108 nm (with a 4× binning), respectively.

SDC: The spinning disc confocal microscope used for imaging the origamis of Fig. 1c and Extended Data Figure 1, was the same system used for the SDC-OPR measurements (CSU-W1 SoRA from Nikon) but the spinning disc was changed for a normal one instead of using the SoRA disc.

Imaging parameters

For DNA-origami imaging, images were taken on the SCD-OPR (CSU-W1 SoRA Nikon system) using 15.000 frames and an integration time of 300 ms. For Fig. 1c and first panel of Fig. 1d, 4× magnification and 4× binning size were used, giving a final pixel size of 108 nm. The 561 nm laser at 100 % power (1.75 mW measured after the objective) was used in conjunction with the 605/52 bandpass filter. For second panel of Fig. 1d, 2× magnification and 2 binning size were used, giving a final pixel size of 78 nm. The 561 nm laser at 100 % power (3 mW measured after the objective). For lower panel of Fig. 1d, 1× magnification and no binning were used, giving a final pixel

size of 108 nm. The 561 nm laser at 100 % power (5 mW measured after the objective). For the images taken in the TIR setup, DNA-origamis were imaged using 20.000 frames and integration time of 100 ms with a power density of 600 W/cm^2 (Extended Data Fig. 3).

For Nup107 imaging, images were taken on the SCD-OPR (CSU-W1 SoRA Nikon system) using 18.000 frames and an integration time of 300 ms 4× magnification and 4 binning size were used, giving a final pixel size of 108 nm (Fig. 1e, Fig 1f and Extended Data Figure 6). The 561 nm laser at 100 % power (1.75 mW measured after the objective) was used in conjunction with the 605/52 bandpass filter. For the images taken in the TIR setup, Nup107 were imaged using 30000 frames and a integration time of 100 ms at a power density of 350 W/cm^2 (Extended Data Figure 7)

For microtubule imaging, images were taken on the SCD-OPR (CSU-W1 SoRA Nikon system) microscope using 17500 number of frames and an integration time of 300 ms. For the images at different penetration depth (Fig. 2b and Fig. 2c) 4× magnification and 4× binning size were used, giving a final pixel size of 108 nm. The 561 nm laser at 100 % power (1.75 mW measured after the objective) was used in conjunction with the 605/52 bandpass filter. For the bigger FOV of Fig. 1a, 1× magnification and no binning were used, giving a final pixel size of 108 nm. The 561 nm laser at 100 % power (5mW after the objective) was used in conjunction with the 605/52 bandpass filter. The entire 9µm height of the cell was imaged sequentially in 1-micron steps.

For Third instar eye discs imaging, images were taken on the SCD-OPR (CSU-W1 SoRA Nikon system) using 18000 frames and an integration time of 300 ms 4× magnification and 4 binning size were used, giving a final pixel size of 108 nm (Fig. 1e, Fig 1f and Extended Data Figure 6). The 561 nm laser at 100 % power (1.75 mW measured after the objective) was used in conjunction with the 605/52 bandpass filter. 60x oil immersion lens magnification was used.

For all imaging conditions on the SDC and SDC-OPR a Nikon 60x Apo NA 1.49 oil immersion lens magnification was used. All imaging parameters can be found in Extended Data Table 1.

Deconvolution

Deconvolution of the SDC-OPR images was performed using NIS-Elements AR. Each image was processed using the blind deconvolution method with 12 iterations.

DNA-PAINT analysis

The raw fluorescence videos were processed for super-resolution reconstruction using the Picasso software package[5] (latest version accessible at

https://github.com/jungmannlab/picasso). Drift correction was applied using redundant cross-correlation, utilizing gold particles as fiducials for cellular experiments.

Localization precision and resolution

In this manuscript, the Cramér Rao lower bound (CRLB) of the single-molecule fit is used to determine the localisation precision values informed (σ_{SMLM}).

$$\sigma_{SMLM} = \sqrt{(\sigma_x)^2 + (\sigma_y)^2}$$

We also provided the localisation precision determined using closest neighbour analysis (NeNA)[16]. Finally, the resolution can be estimated as $2.35\sigma_{SMLM}$. In our example, the best resolution obtained was 10 nm, for the DNA-origami sample measured using the SCD-OPR system at 4× magnification, in line with the super-resolved images obtained as docking pairs separated by 10 nm are resolvable.